# Fatigue Design of Welded Bridge Details for Service Stresses

Kentaro Yamada and Pedro Albrecht, University of Maryland

**An average stress range histogram for truck loads on short-span highway bridges is derived from 106 strain range records reported in the literature. The histogram is used in conjunction with the concept of an equivalent stress range and the allowable constant amplitude stress range values specified by AASHTO to design bridge details for service stresses. Practical application of the method is illustrated with two design examples.**

Highway bridge members are designed statically for the maximum stress due to dead and live loads. The dynamic effect of the live load is considered by adding an impact factor. It is well known, however, that a large number of repeated stress cycles may cause fatigue damage to the structural components at stress levels lower than the allowable maximum stress. A safe fatigue design of the structural components is achieved by limiting the value of the stress range caused by the design live load, including impact.

AASHTO specifications (1, 7), article 1.7.3, fatigue design, give the number of repeated stress cycles for which the bridge must be designed and the allowable stress range depending on the type and location of the detail (Figure 1). The allowable stress range values specified by AASHTO correspond to the 95 percent confidence limit for 95 percent survival of beam specimens tested at constant amplitude stress cycling (5, 6). The number of design load cycles is given by the average daily truck traffic (ADTT) for the traveled artery or the number of expected lane loads.

Fatigue design for truck-induced stress ranges is conservative in two respects. First, loadometer studies and strain history records indicate that few trucks have a gross vehicle weight comparable to that of the design truck. A variety of large but light cargos, partially filled trucks, and empty runs produce a frequency distribution curve for truck weights of concave shape with a peak at about 25 percent of the maximum recorded stress range. This is typical of all bridges surveyed. To assume for purposes of fatigue design that all trucks are fully loaded is safe but very conservative.

A more realistic fatigue design should be based on truck-induced stress histories of variable amplitude, which reflect the actual variation in truck weights. This paper derives an average stress histogram for truck loads on short span highway bridges from published data and shows how it can be used in conjunction with the AASHTO constant amplitude stress range values to design bridge details for service stresses.

Fatigue design is conservative in a second way. Several investigators have matched recorded truck weights with induced strains and have consistently observed lower stresses than those predicted by analysis. This is due mainly to the fact that the various analyses and design rules are conservative. It is not a direct result of fatigue design. However, inasmuch as analysis and design rules may be changed to reduce such discrepancies, it is advisable not to relax the fatigue design specifications.

Special permits may be granted for overloads under the AASHTO operating rating (1, 2). Although a discussion of periodic overload effects on fatigue strength is beyond the scope of this paper, it is helpful to point out that preliminary research findings indicate an enhancement of fatigue life at overload frequencies to which bridges are currently being subjected (25).

## STRESS HISTORY OF HIGHWAY BRIDGES

As a first step toward a more realistic fatigue design of highway bridge components, the frequency distribution of stress ranges induced under service conditions, commonly referred to as stress range histogram, must be known. During the last decade, stress range histograms for truck traffic on 29 bridges on Interstate and U.S. highways in semirural and metropolitan areas were recorded (14 through 23). Detailed descriptive information on the bridges and characteristic features of the 106 individual stress range histograms reported in these references is presented elsewhere (13). A collection of all 106 stress range histograms is given by Yamada and Albrecht (24).

Publication of this paper sponsored by Committee on Steel Bridges.

## Notation

The following symbols are used in this paper:

- ADTT = average daily truck traffic,
- $B_1, B_2$ = regression coefficients for S-N curve,
- $f(x)$ = probability density function for stress range histogram,
- $F_y$ = yield point of material,
- $f_r$ = stress range,
- $f_{r,RMS}$ = root mean square stress range,
- $f_{r,RMC}$ = root mean cube stress range,
- $f_{r,equiv}$ = equivalent stress range,
- $f_{r,max}$ = maximum stress range in stress histogram,
- $f_{r,RO}$ = fatigue limit or runout level of stress range,
- N = fatigue life,
- $N_i$ = fatigue life under applied stress range $f_{ri}$,
- $n_i$ = applied cycles of stress range $f_{ri}$,
- $N_{prop}$ = number of design stress cycles above the fatigue limit,
- $N_{total}$ = total number of cycles,
- $N_{year}$ = design fatigue life in years,
- P = percentage of frequency occurrence from $x = x_{min}$ to $x = 1.0$, and
- $x_{min}$ = ratio of fatigue limit to maximum stress range.

## Bridge Type

A breakdown by type of bridge shows that records were obtained from 16 single-span bridges, 8 three-span continuous bridges, 2 end-anchored bridges, 2 suspended span bridges, and 1 semisuspended span bridge.

Most of the bridges have short spans in which the length between supports varies from 11.6 to 24.4 m (38 to 80 ft). Only five bridges have a span longer than 24.4 m (80 ft): two I-96 bridges over the Grand River in Michigan have spans of 29 and 39.3 m (95 and 128 ft) (14), the Yellow Mill Pond twin bridges on I-95 in Bridgeport, Connecticut, have a span of 34.6 m (113.5 ft) (22), and the Lehigh Canal bridge on US-22 near Bethlehem, Pennsylvania, has a span of 44 m (144 ft) (23).

Rolled sections were used as girders in 20 bridges, of which 19 bridges have welded cover plates. Two bridges with longer spans have welded plate girders (14), and one has riveted plate girders (23). The remaining six bridges are of concrete construction, either reinforced (20) or prestressed (14, 17). In all but 4 of the 23 steel girder bridges (16, 18, 20), the slabs are attached to the girders with shear connectors. The thickness of the concrete deck varies between 15 and 20 cm (6 and 8 in).

## Stress Range Histograms

All recorded strain ranges were converted into stress ranges by multiplying by Young's modulus. The number of stress range events in preselected intervals was counted, and the results were presented in the form of a frequency occurrence distribution.

Most strain range measurements, 77 out of 106, were taken with strain gauges attached to the bottom flange either at midspan or near the end of the cover plates. Records from strain gauges attached to slabs (16), reinforcing bars in the slab (16), and tie plates (23) were not included because they are affected by wheel loads rather than truck loads.

For steel girder bridges the stress range intervals, preselected by the investigators for purposes of data presentation, varied from a minimum of 1.4 MPa (200 lbf/in²) (16) to a maximum of 8.3 MPa (1200 lbf/in²) (23). Most of the histograms (69 out of 87), had stress range intervals between 2.8 and 4.1 MPa (400 and 600 lbf/in²). For concrete girders, a value of approximately 0.28 MPa (40 lbf/in²) was used (14, 17). Two typical histograms with 1.4 and 4.1 MPa (200 and 600 lbf/in²) stress range intervals are shown in Figure 2. They were recorded at the extreme fiber of the bottom flange at the midspan of simple beams.

The maximum stress range value recorded varied from 1.2 MPa for a prestressed concrete girder (17) to 72.4 MPa (180 to 10 500 lbf/in²) measured at the bottom flange of the three-span continuous riveted plate girder (23), as shown in Figure 4. Of the 87 steel girder histograms, 35 had a maximum stress range larger than 34.5 MPa (5000 lbf/in²).

A total of 66 stress range histograms were presented with a cutoff point below which no stress ranges were recorded (17, 20, 21, 22, 23), while the remaining 40 were presented with the lowest interval starting at 0 stress range. Two typical histograms are shown in Figure 3: one with a cutoff point of 4.1 MPa (600 lbf/in²) obtained from a strain gauge attached to the bottom flange at midspan of a simple beam (22) and one without a cutoff point recorded at the one-quarter point of a simple span welded plate girder (14). Although both histograms have the same stress range interval, the one with the cutoff point shows a descending frequency distribution, while the one without the cutoff point shows an ascending-descending frequency distribution shape. The same characteristics can be seen in the stress range histograms shown in Figures 2 and 4. Most cutoff points in the stress range histograms were chosen between 3.1 and 6.9 MPa (450 and 1000 lbf/in²). Only 7 out of 106 stress range histograms had cutoff points greater than 25 percent of the highest stress range.

In spite of the variations in $f_{r,max}$ and cutoff points discussed above, the concavity of the frequency distribution curve from the peak frequency at about 25 percent of $f_{r,max}$ to a low value at $f_{r,max}$ is typical of all histograms. To preserve this characteristic feature and to permit a meaningful comparison, the stress range histograms were nondimensionalized with respect to the maximum stress range $f_{r,max}$, and the lowest quartile was deleted.

A uniform cutoff point at 25 percent was selected for the following reasons:

1. Stress ranges below 25 percent of the highest stress range usually fall below the fatigue limit and, hence, do not contribute to fatigue crack propagation.
2. Stresses induced by partial car lane loads were not recorded although their magnitude would be comparable to that for light trucks.
3. Using a cutoff point at 25 percent prevents insignificant low stress ranges from affecting the cumulative frequency distribution at the higher and significant stress ranges.

All 106 nondimensionalized cumulative frequency distributions were then plotted, as shown in Figure 5, together with the computed average. The average of all 106 histograms is shown in Figure 6 in the form of a histogram. It can be expressed by the following probability density function:

$$f(x) = \begin{cases} -12.0(X - 1.0)^3 + 0.07 & 0.25 \leq x \leq 1.0 \\ 0 & \text{otherwise} \end{cases} \qquad (1)$$

where $x = f_r/f_{r,max}$ is the nondimensional stress range. Equation 1 is also plotted in Figure 6. When equation 1 is used for variable amplitude design, the nondimensionalized stress ranges are multiplied by the maximum stress range obtained from the stress analysis. The

Figure 1. Allowable constant amplitude stress range values for stress categories D and E.

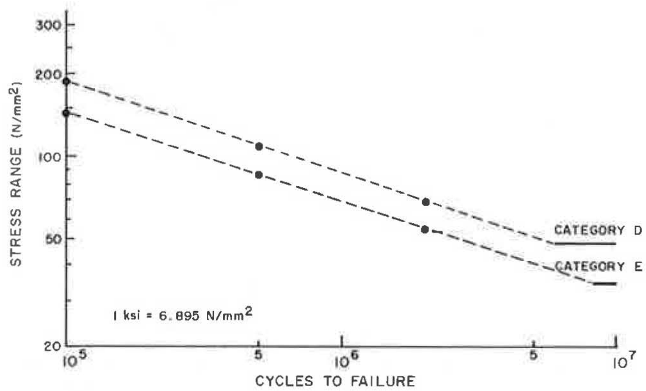


Figure 2. Typical stress range histograms with two extreme stress range intervals.

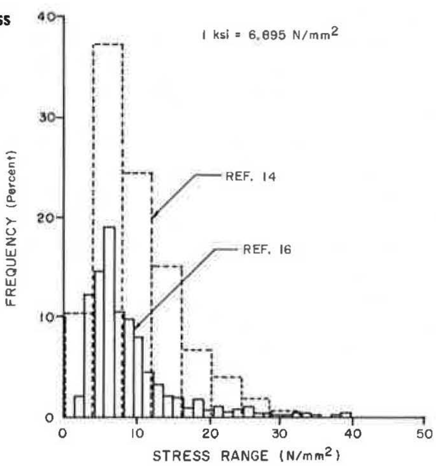


Figure 3. Typical stress range histograms with and without cutoff point.

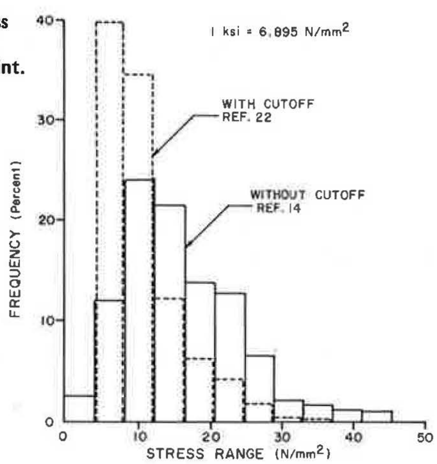


Table 1. RMS and RMC stress range for the average non-dimensionalized stress range histogram.

| Cutoff Point | Percentage Above Cutoff Point | RMS Stress Range (MPa) | RMC Stress Range (MPa) |
|---|---|---|---|
| 0.25 | 100.0 | 0.435 | 0.459 |
| 0.30 | 76.8 | 0.472 | 0.493 |
| 0.40 | 43.0 | 0.551 | 0.566 |
| 0.50 | 22.2 | 0.633 | 0.644 |
| 0.60 | 10.5 | 0.719 | 0.726 |
| 0.70 | 4.5 | 0.806 | 0.810 |
| 0.80 | 1.8 | 0.887 | 0.889 |
| 0.90 | 0.73 | 0.949 | 0.950 |
| 1.00 | 0.0 | 1.0 | 1.0 |

Note: 1 MPa = 145 lbf/in$^2$.

Figure 4. Typical stress range histograms with highest and lowest recorded stress range values, $f_{r,\,max}$.

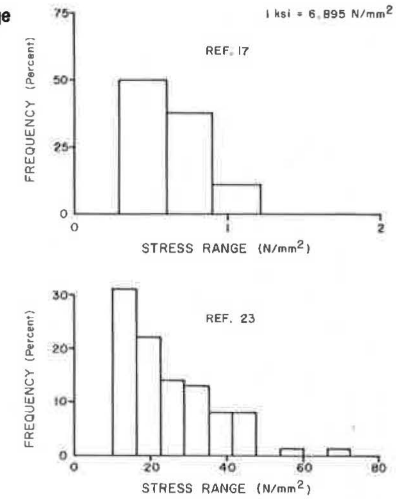


Figure 5. Nondimensional cumulative frequency plot of 106 stress range histograms with cutoff point of 0.25 $f_{r,\,max}$.

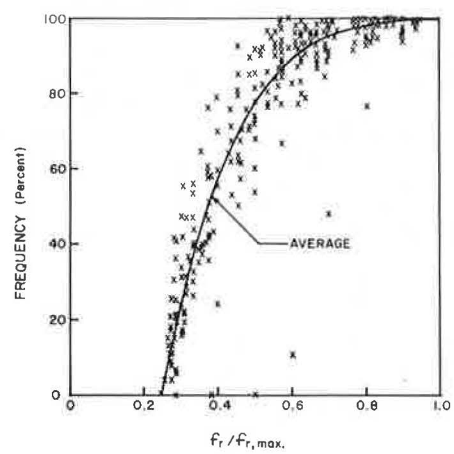


Figure 6. Average nondimensional stress range histogram and probability density function.

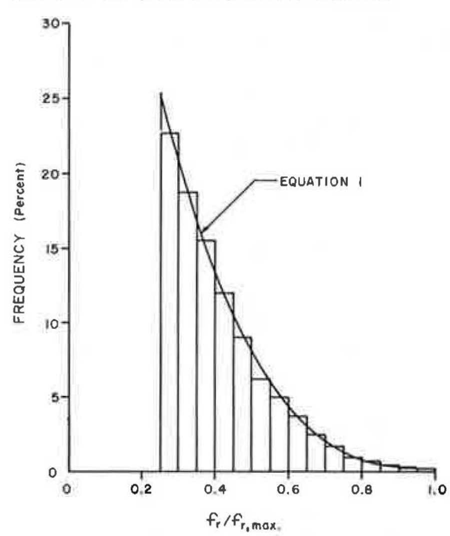

average histogram then accounts for the actual live load variation.

Among the curves investigated for the purpose of best fitting the average cumulative frequency distribution, shown as a step function in Figure 6, were Rayleigh functions. They have been used by others (10), presumably because they follow in general the ascending-descending shape of individual histograms such as those shown in Figure 2. The results of the least squares fit analysis revealed a significant lack of correlation for the Rayleigh curve. Its applicability appears to be questionable also for conceptual reasons. A Rayleigh curve would predict gradually vanishing frequencies at very low loads, where in reality the addition of groups of cars capable of producing comparable stress fluctuations would cause an upward turn in the frequency distribution. Further, retaining the very low stress ranges reduces the equivalent stress range, as discussed below, and leads to nonconservative estimates of variable amplitude fatigue life.

## FATIGUE LIFE PREDICTION

The fatigue life of structural components consists of a crack initiation phase and a crack propagation phase. Severe stress concentrations at weldments and the existence of microcracks and slag inclusions at weld borders tend to reduce the crack initiation phase to a small number of cycles compared with the total fatigue life. Therefore, the initiation phase is usually neglected, and the analysis of the useful life is based on crack propagation alone. The assumption is conservative for purposes of design and indeed necessary because undesired weld cracking can preempt entirely the initiation phase.

### Stress Range Versus Fatigue

The constant amplitude fatigue life of weldments is determined experimentally. The data are usually presented as a log-log plot of stress range versus fatigue life (S-N) with the mean life given by

$$\text{Log } N = B_1 + B_2 \log f_r \tag{2}$$

$B_1$ and $B_2$ are regression coefficients obtained from a least squares fit. The AASHTO specifications (1) classify all structural details in five stress categories, A through E, according to their fatigue resistance. For each stress category, the constant amplitude stress range is specified as a function of the design life on the basis of the 95 percent confidence limit for 95 percent survival obtained from the statistical analysis of the pertinent test data. For example, allowable stress ranges for stress categories C and D(1) are shown by the solid points and lines in Figure 1.

At low values of stress range, a fatigue limit or a runout level exists for each detail below which fatigue cracking will not occur even after application of a large number of load cycles, usually on the order of 10 million. The safe fatigue limit for details in stress categories C and D is shown by solid lines in Figure 1.

### Equivalent Constant Amplitude Stress Range

Recently, the concept of an equivalent constant amplitude stress range has been advanced (10). It is defined as the constant amplitude stress range that will give the same fatigue life as the variable amplitude stress history. Barsom (3) successfully used the root mean square stress range, $f_{r,RMS}$, to correlate fatigue crack propagation rates under constant and variable amplitude cycling.

The RMS stress range is defined as the square root of the mean sum of squares of all stress ranges:

$$f_{r,RMS} = \left(\sum_{i=1}^{s} n_i f_{ri}^2 \Big/ N\right)^{1/2} \tag{3}$$

where

$N$ = total number of cycles,
$s$ = number of stress range levels, and
$n_i$ = number of stress range cycles at each level.

Equation 3 can be derived from the condition that the strain energy induced by a total of N variable amplitude stress cycles must be the same as the strain energy caused by the application of N stress cycles of constant amplitude, $f_{r,RMS}$.

Combining Miner's theory with the S-N curves fitted to fatigue test data suggests, however, that an exponent of 3 rather than 2 should be used in equation 3. This is shown below.

The Palmgren-Miner theory (8) is an empirical, cumulative damage criterion for evaluation of variable amplitude fatigue life. Its widespread use can be attributed to both the simplicity of the method and the ease of application. The Palmgren-Miner theory states that the damage caused by a number of stress cycles, $n_i$, can be expressed as a fraction of $n_i$ to the number of cycles, $N_i$, required to fail the component at the same stress range level. Failure occurs when the summation of the fractions for each level adds up to unity.

$$\sum_{i=1}^{s}(n_i/N_i) = 1.0 \tag{4}$$

By substituting the anti-log of equation 2 into equation 4, the Palmgren-Miner criterion is given by

$$\sum_{i=1}^{s}(n_i/10^{B_1} f_{ri}^{B_2}) = 1.0 \tag{5}$$

If the equivalent constant amplitude stress range, $f_{r,equiv}$, causes failure, the life, N, can be expressed by the anti-log of equation 2 as

$$N = 10^{B_1} f_{r,equiv}^{B_2} \qquad (Nf_{r,equiv}^{-B_2}/10^{B_1}) = 1.0 \tag{6}$$

Equating the identities expressed by equations 5 and 6 and solving for the equivalent stress range yield

$$f_{r,equiv} = \left(\sum_{i=1}^{s} n_i f_{ri}^{-B_2} \Big/ N\right)^{-(1/B_2)} \tag{7}$$

Equation 7 is of the same form as equation 3 except the exponent is different. If $-B_2 = 3$, as found for most structural details (5, 6), is substituted, the equivalent stress range is given by a so-called root mean cube stress.

$$f_{r,RMC} = \left[\sum_{i=1'}^{s}(n_i f_{ri}^3/N)\right]^{1/3} \tag{8}$$

As previously explained, a runout level of stress range, $f_{r,RO}$ (also called fatigue or endurance limit) is assumed when a large number of cycles, usually on the order of 10 million, do not produce any fatigue cracking. Therefore the stress range levels below the fatigue limit should be deleted from the calculation of RMS or RMC stresses. Root mean square and root mean cube stresses for the average stress range histogram, equation 1, were computed for several values of fatigue limit, expressed as a fraction of the maximum stress range. The results are given in Table 1. For example, if the fatigue limit of a given detail is 50 percent of the maximum design stress range, only 22.2 percent of all trucks cause stress ranges above the fatigue limit, and its RMS and RMC stress ranges are given by 0.633 and 0.644 of $f_{r,max}$. The difference between the RMS and RMC stress ranges is approximately 5 percent when $f_{r,RO} = 0.25\ f_{r,max}$ and decreases further as the relative fatigue limit increases.

These small differences explain partially why good correlation between constant and variable amplitudes test data can be obtained by plotting the fatigue lives against the root mean square stress range. The RMC stress range is based, however, on a sounder theoretical and experimental foundation.

## The Fracture Mechanics Approach

In contrast to Miner's empirical theory, the fracture mechanics approach is based on the physical phenomena of fatigue crack propagation. It has been used with success to correlate observed fatigue lives with the computed number of cycles required to propagate a fatigue crack from an average initial size to failure, for both constant and variable amplitude fatigue. It also explains why the slope of all S-N curves is the same and about numerically equal to the slope of curves in log-log plots of crack growth rate versus range of stress intensity factor. The value of the slope is about 3 for structural details and steels.

It can be shown that both Miner's theory (equation 4) and the root mean cube stress range concept (equation 8) are special cases of the fracture mechanics approach. They give identical variable amplitude fatigue life prediction (13) provided that (a) the crack initiation phase is negligible, (b) no interaction exists between the stress range levels, (c) only stress ranges above the fatigue limit are retained, and (d) the slopes of the S-N curves and the crack growth rate curves are about 3. Substantial experimental evidence can be presented in support of each one of the four conditions.

## APPLICATION

A more realistic fatigue design of welded bridge details for service stresses can be performed with the aid of (a) an average stress range histogram for highway bridges, (b) the concept of an equivalent stress range, and (c) the allowable constant amplitude stress range values specified by AASHTO. The following design procedure is recommended.

1. Find the maximum stress range, $f_{r,max}$, at the detail due to live load and impact.
2. Compute $x_{min} = f_{r,RO}/f_{r,max}$, where the runout stress range, $f_{r,RO}$, is defined in the AASHTO specifications (more than 2 million cycles).
3. Find the equivalent RMC stress range, $f_{r,RMC}$.
4. Compute the percentage of frequency occurrence, P, of the stress cycles above the fatigue limit by integrating the probability density function, f(x), from $x = x_{min}$ to $x = 1.0$. This is the percentage of stress range cycles that contribute to crack propagation. Alternatively read the RMC stress range directly from Table 1.
5. From the S-N plot for the appropriate stress category, read the propagation life, $N_{prop}$, corresponding to the equivalent stress range, $f_{r,RMC}$ (Figure 1).
6. Divide the propagation life, $N_{prop}$, by the percentage of frequency occurrence to obtain the total truck traffic, $N_{total} = N_{prop}/P$.
7. Compute the expected fatigue life in calendar years from $N_{year} = N_{total}/(360 \times ADTT)$.

## REFERENCES


1. Standard Specifications for Highway Bridges. AASHTO, 1974.
2. Manual for Maintenance and Inspection of Bridges. AASHTO, 1976.
3. J. M. Barsom. Fatigue-Crack Growth Under Variable-Amplitude Loading in ASTM A514-B Steel. ASTM, Special Technical Publ. STP 536, 1973, pp. 147-167.
4. T. R. Gurney. Fatigue of Welded Structures. Cambridge Press, 1968.
5. J. W. Fisher, K. H. Frank, M. A. Hirt, and B. M. McNamee. Effect of Weldments on the Fatigue Strength of Steel Beams. NCHRP, Rept. 102, 1970.
6. J. W. Fisher, P. A. Albrecht, B. T. Yen, D. J. Klingerman, and B. M. McNamee. Fatigue Strength of Steel Beams With Welded Stiffeners and Attachment. NCHRP, Rept. 147, 1974.
7. J. W. Fisher. Guide to 1974 AASHTO Fatigue Specifications. American Institute of Steel Construction, 1974, pp. 29-31.
8. M. A. Miner. Cumulative Damage in Fatigue. Journal of Applied Mechanics, Trans., ASME, Vol. 67, Sept. 1945, pp. A-159—A-164.
9. W. H. Munse. Fatigue of Welded Steel Structures. Welding Research Council, 1964.
10. C. G. Schilling, K. H. Klippstein, and R. J. Reilly. Simulated Traffic Fatigue Loading of Steel Bridges. Preprint, Specialty Conference on Metal Bridges, ASCE, Nov. 1974, pp. 379-410.
11. J. E. Stallmeyer and W. H. Walker. Cumulative Damage Theories and Application. Journal of Structural Division, Proc., ASCE, Vol. 94, No. ST12, Dec. 1968, pp. 2739-2750.
12. J. P. Tang and J. T. P. Yao. Random Fatigue-Literature Review. Univ. of New Mexico, Albuquerque, Technical Rept. CE-22(70) NSF-065, July 1970.
13. K. Yamada. Fatigue Behavior of Structural Components Subjected to Variable Amplitude Loading. Univ. of Maryland, College Park, PhD dissertation, 1975.
14. G. R. Cudney. The Effects of Loadings on Bridge Life. Michigan Department of State Highways, Research Rept. R-638, Sept. 1967.
15. T. R. Douglas and J. B. Karrh. Fatigue Life of Bridges Under Repeated Highway Loading. Alabama Highway Research, HPR Rept. 54, April 1971.
16. C. P. Heins and A. D. Sartwell. Tabulation of 24 Hours Dynamic Strain Data on Four Simple Span Girder-Slab Bridge Structures. Civil Engineering Department, Univ. of Maryland, College Park, Progress Rept. 29, June 1969.
17. W. T. McKeel, C. E. Maddox, H. L. Kinnier, and C. F. Galambos. A Loading History Study of Two Highway Bridges in Virginia. Virginia Highway Research Council, Charlottesville, Final Rept. VHRC 70-R48, June 1971.
18. D. C. Sartwell and C. P. Heins. Tabulation of Dynamic Strain Data on a Girder Slab Bridge Structure During Seven Continuous Days. Civil Engineering Department, Univ. of Maryland, College Park, Progress Rept. 31, Sept. 1969.

19. A. D. Sartwell and C. P. Heins. Tabulation of Dynamic Strain Data on a Three Span Continuous Bridge Structure. Civil Engineering Department, Univ. of Maryland, College Park, Progress Rept. 33, Nov. 1969.
20. D. W. Goodpasture. Stress History of Highway Bridges. Department of Civil Engineering, Univ. of Tennessee, Dec. 1972.
21. P. O. Christiano and L. E. Goodman. Bridge Stress Range History. HRB, Highway Research Record 382, 1972.
22. D. G. Bowers. Loading History of Span 10 on Yellow Mill Pond Viaduct. HRB, Highway Research Record 428, 1973, pp. 64-71.
23. J. W. Fisher, B. T. Yen, and N. V. Marchica. Fatigue Damage in the Lehigh Canal Bridge. Fritz Engineering Laboratory, Lehigh Univ., Bethlehem, Penn., Rept. 386.1, Nov. 1974.
24. K. Yamada and P. A. Albrecht. A Collection of Live Load Stress Histograms of U.S. Highway Bridges. Univ. of Maryland, College Park, Civil Engineering Rept., 1975, pp. 39-144.
25. P. Albrecht, A. Abtahi, and G. R. Irwin. Fatigue Strength of Overloaded Bridge Components. Univ. of Maryland, College Park, Civil Engineering Rept., 1975.